

Reversible gas-phase redox processes catalyzed by Co-exchanged MFU-4l(arage)

Dmytro Denysenko, Tamas Werner, Maciej Grzywa, Angela Puls, Volker Hagen, Georg Eickerling, Jelena Jelic, Karsten Reuter, Dirk Volkmer

Angaben zur Veröffentlichung / Publication details:

Denysenko, Dmytro, Tamas Werner, Maciej Grzywa, Angela Puls, Volker Hagen, Georg Eickerling, Jelena Jelic, Karsten Reuter, and Dirk Volkmer. 2012. "Reversible gas-phase redox processes catalyzed by Co-exchanged MFU-4l(arage)." *Chemical Communications* 48 (9): 1236–38. <https://doi.org/10.1039/c2cc16235k>.

Nutzungsbedingungen / Terms of use:

licgercopyright

Dieses Dokument wird unter folgenden Bedingungen zur Verfügung gestellt: / This document is made available under these conditions:

Deutsches Urheberrecht

Weitere Informationen finden Sie unter: / For more information see:

<https://www.uni-augsburg.de/de/organisation/bibliothek/publizieren-zitieren-archivieren/publiz/>



Reversible gas-phase redox processes catalyzed by Co-exchanged MFU-4l(arge)[†]

Dmytro Denysenko,^a Tamas Werner,^a Maciej Grzywa,^a Angela Puls,^b Volker Hagen,^c Georg Eickerling,^d Jelena Jelic,^e Karsten Reuter^e and Dirk Volkmer^{*a}

Postsynthetic metal ion exchange in a benzotriazolate-based MFU-4l(arge) framework leads to a Co(II)-containing framework with open metal sites showing reversible gas-phase oxidation properties.

Metal–organic frameworks have been suggested for a number of applications such as heterogeneous catalysis, gas storage, gas separation and drug delivery.¹ With respect to catalytic applications MOFs possessing highly accessible, redox active metal centers are particularly interesting.² However, besides sustained catalytic activity, production scale applications require processable (*i.e.* moldable) catalyst particles that are solvolytically stable and mechanically robust, and these anti-tethic requirements seem to drastically limit the number of suitable coordination frameworks. Identifying novel MOF structural families of potential use in catalytic applications thus represents the first and foremost step, preceding further development towards technical applications.³

Aiming at MOF oxidation catalysts we have recently reported on MFU-1, which is a cobalt-based structural analogue of MOF-5.⁴ Solution impregnation of MFU-1 with a co-catalyst (*N*-hydroxyphthalimide) leads to NHPI@MFU-1, which oxidizes a range of organic substrates under ambient conditions by employing molecular oxygen from air.⁵ However, attempts to replace the Co²⁺ ions in MFU-1 by other redox active metal centers as yet were unsuccessful. To overcome this limitation, we here present the first example of a novel redox active MOF, which is derived from MFU-4l(arge)⁶—a recent member of the highly modular and robust MFU-4 structural family.⁷ MFU-4 type frameworks are based on pentanuclear *T_d* symmetrical [Zn^{II}Zn₄Cl₄(ta)₆] coordination units (o—octahedral, t—tetrahedral

metal coordination sites, ta—triazolate ligand). In MFU-4-type frameworks rigid benzobistriazolate linkers (BBTA²⁻) occupy the positions of the triazolate (ta) moieties.

MFU-4l, constructed from deprotonated bis(1*H*-1,2,3-triazolo-[4,5-*b*],[4',5'-*b'*])dibenzo-[1,4]-dioxin (H₂-BTDD) linkers, constitutes a highly porous framework with large pore apertures (av. dia. 9.1 Å) and coordinatively unsaturated metal coordination sites. Heating up a MFU-4l suspension/CoCl₂ solution in DMF leads to isostructural replacement of zinc by Co(II) centres (Fig. 1). Depending on the Co/Zn molar ratio of the initial suspension, the total number *x* of Co(II) replacing zinc in the formula unit [Co_{*x*}Zn_(5-*x*)Cl₄(BTDD)₃] may differ (Fig. 2). It is clearly seen that the Co/Zn exchange process follows a sigmoidal behaviour: at a Co/Zn molar ratio < 0.3 (inset of Fig. 2) the exchange curve indicates a substoichiometric replacement of zinc centers. In order to reach *x* = 1 (*i.e.* on average one Co(II) center per pentanuclear SBU) the initial Co/Zn molar ratio of the suspension has to be adjusted to a value of about 0.30 ± 0.02. The complete exchange of zinc centers requires a huge excess of cobalt ions in the

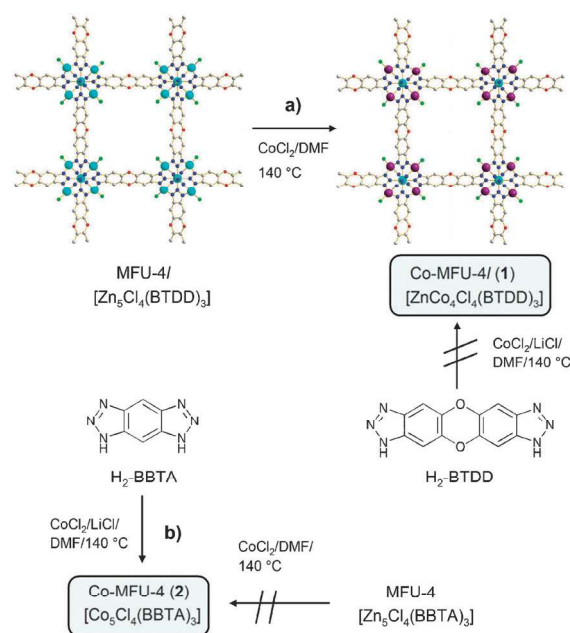


Fig. 1 Synthesis of **1** via postsynthetic Co/Zn metal exchange (a) and direct synthesis of **2** (b).

^a Institute of Physics, Chair of Solid State and Material Science, Augsburg University, D-86135 Augsburg, Germany.

E-mail: dirk.volkmer@physik.uni-augsburg; Fax: + 49 (0)821 598-5955

^b Rubotherm GmbH, D-44799 Bochum, Germany

^c Rubokat GmbH, D-44801 Bochum, Germany

^d Institute of Physics, Chair of Chemical Physics and Material Science, Augsburg University, D-86135 Augsburg, Germany

^e Dept. Chemie, Technische Universität München, D-85747 Garching, Germany

[†] Electronic supplementary information (ESI) available: Experimental details, spectral data, TGA data, XRPD data and crystal structure data. CCDC 847582 (1), CCDC 847583 (2) and CCDC 847498 (3). For ESI and crystallographic data in CIF or other electronic format see

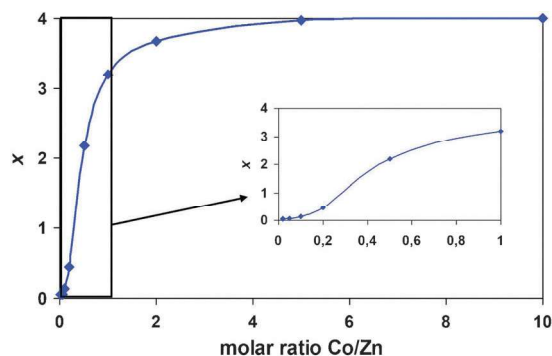


Fig. 2 Total number x of Co(II) ions per $\{\text{Co}_x\text{Zn}_{5-x}\text{Cl}_4\}^{6+}$ unit as a function of (Co/Zn) molar ratio under solvothermal reaction conditions, determined by energy-dispersive X-ray spectroscopy (EDX).

suspension (Co/Zn molar ratio > 5). It should be noted that the exchange curve (Fig. 2) converges towards a plateau at $x = 4$ (and not 5!), suggesting that the central octahedrally coordinated Zn center cannot be replaced using the given experimental conditions. Thus, the average chemical formula of cobalt-exchanged MFU-4l may be formulated as $[\text{Zn}^0(\text{Co}_x\text{Zn}_{4-x})\text{Cl}_4(\text{BTDD})_3]$ (**1**).

In contrast to these findings, the Co/Zn metathesis starting from MFU-4 failed completely, which is probably due to strong diffusion limitations imposed on solvated metal ions, caused by the very small pore apertures (av. dia. 2.5 Å) of this framework.⁷ However, in contrast to **1** an isostructural MFU-4 derivative, termed Co-MFU-4 (**2**), was directly prepared from 1*H*,5*H*-benzo(1,2-*d*:4,5-*d'*)bistriazole (H_2 -BBTA) and CoCl_2 in DMF in the presence of LiCl under solvothermal reaction conditions, a reaction path that proved unsuccessful in the case of **1** (Fig. 1). Based on powder X-ray diffraction data the crystal structures of both Co-containing frameworks have been refined by the Rietveld method, starting from structural models of the isostructural compounds MFU-4 and MFU-4l, respectively (Table 1). Both MOF compounds (**1** and **2**) are thermally stable (up to 450 °C under nitrogen atmosphere), as confirmed by TGA and VT-XRPD analysis. Compound **1** is highly porous with a BET surface area of 3556 m² g^{−1} (Table 1).

In order to ensure that the tetrahedral coordination geometry of the Co(II) centers in **1** and **2** is retained, the discrete pentanuclear “Kuratowski-type” complex⁸ of formula $[\text{Co}^0\text{Co}_4\text{Cl}_4(\text{Me}_2\text{bta})_6]\cdot 2\text{PhBr}$ (**3**, Me_2bta = 5,6-dimethylbenzotriazolate) has been prepared, serving as structural and spectroscopic model of SBUs that are present in **1** and **2**. Its structure has been solved from single crystal X-ray data. Compound **3** crystallizes in the cubic crystal system, space group $Fd\bar{3}m$; it is isostructural with the zinc complex described previously.^{8a} An ORTEP style plot of the asymmetric unit of **3** with atom labels and bond lengths is shown in Fig. 3.

The diffuse reflectance UV/vis spectra of compounds **1–3** show strong absorption bands at ca. 600 nm, typical for Co(II) centers in tetrahedral coordination environments, and corresponding to the spin-allowed $^4\text{A}_2(\text{F}) \rightarrow ^4\text{T}_1(\text{P})$ transition. Ligand field splitting energies Δ_{t} (Co^{2+}) and Racah parameters B_{t} (Co^{2+}), calculated from the Tanabe–Sugano diagram for tetrahedrally coordinated d⁷ metal ions, are similar for all compounds, where **2** has the highest splitting energy. IR spectra

Table 1 Selected features and crystallographic data for compounds **1–3** containing Kuratowski-type coordination units

Compound	1	2	3
Chemical formula	$\text{C}_{36}\text{H}_{12}\text{Cl}_4$ $\text{Co}_4\text{N}_{18}\text{O}_6\text{Zn}$	$\text{C}_{18}\text{H}_6\text{Cl}_4$ Co_5N_{18}	$\text{C}_{60}\text{H}_{38}\text{Br}_2\text{Cl}_4$ Co_5N_{18}
Formula weight (M)	1235.5	910.8	1627.5
T/K	293(2)	293(2)	100(1)
Crystal system	Cubic	Cubic	Cubic
Space group	$Fd\bar{3}m$ (225)	$Fd\bar{3}m$ (225)	$Fd\bar{3}m$ (227)
Cell length $a = b = c/\text{\AA}$	30.9950(7)	21.7309(4)	23.5130(1)
Unit cell volume/ \AA^3	29776.6(7)	10262.1(2)	12999.42(10)
Z	8	8	8
Reflections total	—	—	28354
Reflections unique	—	—	999
$R_{\text{int}}(F)$	—	—	0.066
$R_1(I(F_o)) > 2\sigma(I)$	—	—	0.0358
wR_2 (all data)	—	—	0.0885
$F(000)$	4768	3501	5320
Reflections observed	86	55	—
Number of observ.	4300	4300	—
R_{p}	1.38	1.30	—
R_{wp}	2.25	1.82	—
R_{wobs}	6.08	13.97	—
Diameter A-cells/ \AA	11.97	4.43	—
Diameter B-cells/ \AA	18.52	11.97	—
Aperture/ \AA	9.14	2.98	—
BET surface area, m ² g ^{−1} (Ar, 77 K)	3556	1435	—
λ_{max} (Co^{2+})/nm	605	609	624
Δ_{t} (Co^{2+})/cm ^{−1}	4016	4201	3797
B_{t} (Co^{2+}), cm ^{−1}	762	737	747
Vibrational mode including Co–Cl stretch (FTIR)/cm ^{−1}	383	415	372

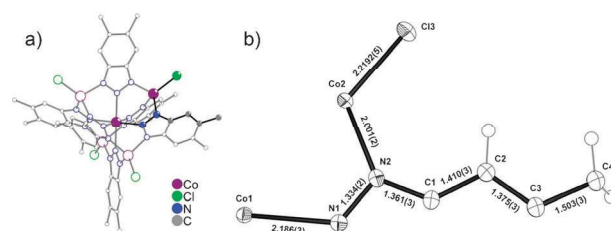


Fig. 3 Structure of **3** (a) and an asymmetric unit of **3** (b). Atoms represented by ORTEP style thermal ellipsoids (50% probability).

recorded at the wavenumber range from 600–180 cm^{−1} show characteristic vibrational modes: out of these, the Co–Cl single bond stretching mode could be unequivocally assigned based on comparison with spectroscopic data gleaned from DFT calculations on **3**. The DFT calculations were performed with the full-potential code FHI-aims,⁹ using the GGA–PBE functional¹⁰ to describe electronic exchange and correlation, a tier2 basis set and tight integration settings.

Selected structural and spectroscopic data of compounds **1–3** are given in Table 1.

In summary the structural and spectroscopic data provide sound evidence for the fact that all three compounds possess coordinatively unsaturated Co(II) centers in the (N₃Cl) donor environment typical of Kuratowski-type units.

As a proof-of-concept the gas phase redox activity of MOF compounds **1** and **2** has been investigated by cyclic temperature-programmed oxidation (TPO) and reduction (TPR) monitored by an online mass spectrometer. The TPO curve of **1** shows reversible oxidation with molecular oxygen around approx. 80 °C, whereas **2** shows no oxidation under identical conditions

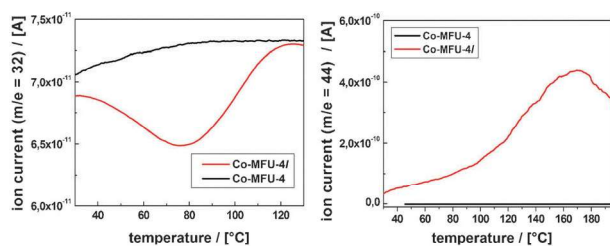


Fig. 4 Left: TPO curves; right: CO-TPSR curves for **1** and **2**.

(Fig. 4, left). Reversibility of these gas phase redox processes has been confirmed by repeating all TPR/TPO experiments for at least three times. Mass spectra concomitantly recorded during O₂ exposition gave no indication of volatile compounds being formed during oxidation of **1** at 80 °C, which suggests a stoichiometric uptake (*i.e.* coordination) of O₂ by Co²⁺ ions. At higher temperatures (not shown) a decomposition of the organic framework indicated by a significant evolution of CO₂ and water is indicated.

The TPSR (Temperature Programmed Surface Reaction) technique is a suitable method to prove if an adsorbed species (*e.g.* oxygen during TPO) is capable of catalytic (oxidation) reaction. CO oxidation is probably the simplest reaction to indicate if the adsorbed oxygen is also reactive for oxidation reactions. The samples were pretreated during heating in oxygen flow (1000 ppm in He) up to 200 °C and subsequent cooling in the same gas mixture to ambient. Afterwards the samples have been flushed with helium under ambient conditions. The experimental data were recorded during a linear heat-up in a 10% CO/He mixture. **1** shows a significant trace of CO₂ ($m/e = 44$) while **2** shows no indication for CO₂ formation (Fig. 4, right). This result is clearly corresponding to the observed reversible oxidation behaviour of the two samples. It can be concluded that the open framework structure of the Co-MFU-4l sample ensures a sufficient accessibility of catalytically active Co centres, whereas Co-MFU-4, albeit containing similar SBUs, is catalytically inactive owing to hindered diffusion/transport of gas molecules. The reaction temperature range is considerably higher than the one reported for Co₃O₄ nanoparticles (−77 °C). However, CO oxidation catalysts containing Co₃O₄ usually require much higher pre-treatment temperatures (450–550 °C),¹¹ whereas in the case of **1** 200 °C is sufficient for catalyst activation. This points to an advantage of the new MOF compound **1** compared to conventional cobalt oxide-based catalysts and shows its potential as a heterogeneous catalyst for gas phase reactions.

A few examples of postsynthetic metal exchange in MOFs have been reported by now, such as the partial exchange of Zn²⁺ by Co²⁺ in MOF-5¹² and some others.¹³ We demonstrate here that isostructural replacement of Zn²⁺ ions in

MFU-4 type frameworks leads to redox active Co(II) derivatives featuring catalytically active metal sites. Postsynthetic metal metathesis therefore may offer a general approach toward redox active frameworks comprising coordinatively unsaturated metal centers that might be difficult to obtain *via* direct synthesis from their components.

Comparative TPO/TPSR studies on **1** and **2** show that only **1** has accessible metal centers that undergo multiple and reversible redox reactions in gas phase TPO and TPR cycles. The striking lack of a similar redox activity in **2** is ascribed to its narrow pore size which limits gas diffusion within the pore volume of this particular MOF. To our understanding Co-MFU-4l represents a novel prototypic MOF which comprises all essential properties (*i.e.* redox reversibility, thermal stability, robustness) required for the future development of MOF catalysts suitable for gas phase heterogeneous redox processes.

Notes and references

- (a) G. Feréy, *Chem. Soc. Rev.*, 2008, **37**, 191–214; (b) Z. Ma and B. Moulton, *Coord. Chem. Rev.*, 2011, **255**, 1623–1641.
- V. Colombo, S. Galli, H. J. Choi, G. D. Han, A. Maspero, G. Palmisano, N. Masciocchi and J. R. Long, *Chem. Sci.*, 2011, **2**, 1311–1319.
- J. Lee, O. K. Farha, J. Roberts, K. A. Scheidt, S. T. Nguyen and J. T. Hupp, *Chem. Soc. Rev.*, 2009, **38**, 1450–1459.
- M. Tonigold, Y. Lu, B. Bredenkötter, B. Rieger, S. Bahn Müller, J. Hitzbleck, G. Langstein and D. Volkmer, *Angew. Chem.*, 2009, **121**, 7682–7687.
- M. Tonigold, Y. Lu, A. Mavrandonakis, A. Puls, R. Staudt, J. Möllmer, J. Sauer and D. Volkmer, *Chem.–Eur. J.*, 2011, **17**, 8671–8695.
- D. Denysenko, M. Grzywa, M. Tonigold, B. Streppel, I. Krkljus, M. Hirscher, E. Mugnaioli, U. Kolb, J. Hanss and D. Volkmer, *Chem.–Eur. J.*, 2011, **17**, 1837–1848.
- S. Biswas, M. Grzywa, H. P. Nayek, S. Dehnen, I. Senkovska, S. Kaskel and D. Volkmer, *Dalton Trans.*, 2009, 6487–6495.
- (a) S. Biswas, M. Tonigold and D. Volkmer, *Z. Anorg. Allg. Chem.*, 2008, **634**, 2532–2538; (b) S. Biswas, M. Tonigold, M. Speldrich, P. Kögerler, M. Weil and D. Volkmer, *Inorg. Chem.*, 2010, **49**, 7424–7434; (c) Y.-Y. Liu, M. Grzywa, M. Tonigold, G. Sastre, T. Schüttigkeit, N. S. Leeson and D. Volkmer, *Dalton Trans.*, 2011, **40**, 5926–5938.
- V. Blum, R. Gehrke, F. Hanke, P. Havu, V. Havu, X. Ren, K. Reuter and M. Scheffler, *Comput. Phys. Commun.*, 2009, **180**, 2175–2196.
- J. P. Perdew, K. Burke and M. Ernzerhof, *Phys. Rev. Lett.*, 1996, **77**, 3865–3868.
- (a) J. Jansson, A. E. C. Palmqvist, E. Fridell, M. Skoglundh, L. Österlund, P. Thormählen and V. Langer, *J. Catal.*, 2002, **211**, 387–397; (b) X. Xie, Y. Li, Z.-Q. Liu, M. Haruta and W. Shen, *Nature*, 2009, **458**, 746–749.
- J. A. Botas, G. Calleja, M. Sánchez-Sánchez and M. G. Orcajo, *Langmuir*, 2010, **26**, 5300–5303.
- (a) M. Dincă and J. R. Long, *J. Am. Chem. Soc.*, 2007, **129**, 11172–11176; (b) L. Mi, H. Hou, Z. Song, H. Han, H. Xu, Y. Fan and S.-W. Ng, *Cryst. Growth Des.*, 2007, **7**, 2553–2561; (c) L. Mi, H. Hou, Z. Song, H. Han and Y. Fan, *Chem.–Eur. J.*, 2008, **14**, 1814–1821; (d) S. Das, H. Kim and K. Kim, *J. Am. Chem. Soc.*, 2009, **131**, 3814–3815; (e) T. K. Prasad, D. H. Hong and M. P. Suh, *Chem.–Eur. J.*, 2010, **16**, 14043–14050.